



A homotopy perturbation method for fractional-order advection-diffusion-reaction boundary-value problems



I. Ateş*, P.A. Zegeling

Department of Mathematics, Utrecht University, Budapestlaan 6, 3584 TD Utrecht, The Netherlands

ARTICLE INFO

Article history:

Received 20 January 2016

Revised 1 February 2017

Accepted 6 March 2017

Available online 10 March 2017

Keywords:

Fractional boundary-value problems

Homotopy perturbation method

Adomian decomposition method

Bratu model

advection-diffusion-reaction

Boundary layers

Caputo derivative,

ABSTRACT

In this paper we describe the application of the homotopy perturbation method (HPM) to two-point boundary-value problems with fractional-order derivatives of Caputo-type. We show that HPM is equivalent to the semi-analytical Adomian decomposition method when applied to a class of nonlinear fractional advection-diffusion-reaction models. A general expression is derived for the coefficients in the HPM series solution. Numerical experiments are given to demonstrate several properties of HPM, such as its dependence on the fractional order and the parameters in the model. In the case of more than one solution, HPM has difficulties to find the second solution in the model. Another example is given for which HPM seems to converge to a non-existing solution.

© 2017 Elsevier Inc. All rights reserved.

1. Introduction

This paper is devoted to the analytical and numerical study of a semi-analytical technique known as the homotopy perturbation method (HPM). The method was introduced by He [1–4]. For general nonlinear boundary-value models, it is almost impossible to derive exact solutions. Even if they are available, the calculations to obtain numerical values may be cumbersome, or it may be difficult to interpret the behavior of the solution. HPM couples the traditional perturbation method and homotopy in topology. This gives HPM a significant advantage to obtain an approximate solution to a wide range of nonlinear problems. The method provides rapid convergent series solutions in most of the cases. Usually, already a few iterations result in a high accurate solution. Recently, several new approximation methods in terms of infinite series have been proposed. These methods include the Adomian decomposition method [5], the variational iteration method [6], the *Exp*-function method [7], homotopy analysis method (HAM) [8,9] and HPM. Recent papers on HPM use local fractional operators [10,11] and apply HPM to engineering problems [12,13]. HAM is a more general version of HPM and it gives the HPM solution for a particular choice of the HAM parameter \hbar . The present paper is devoted to the analysis and application of HPM to a class of fractional-order boundary-value problems.

2. A fractional-order advection-diffusion-reaction model

In literature, many definitions of the fractional derivative have been proposed. The most common definitions of fractional calculus are the Riemann–Liouville, Grünwald–Letnikov and Caputo definitions [14–16]. Recently, three other definitions have been introduced [17–19].

* Corresponding author.

E-mail addresses: I.Ates@uu.nl, inanates@gmail.com (I. Ateş).

We consider the following fractional-order BV-model of Bratu-type with damping and source term [20–22]

$$\begin{cases} \in \mathcal{D}_C^\alpha u + \gamma u' + f(u) = S(x), & x \in [0, 1], \\ u(0) = u_L, & u(1) = u_R, \end{cases} \quad (1)$$

with parameters $1 < \alpha \leq 2$, $0 < \epsilon \leq 1$, and $\gamma \in \mathbb{R}$. The nonlinear source term $f: [0, \infty) \rightarrow [0, \infty)$ is assumed to be continuous. The function $S(x)$ represents a spatially dependent source term. The solution u is a function $u: [0, 1] \rightarrow [0, \infty)$. Applications stem, among others, from astrophysics and combustion theory. With \mathcal{D}_C^α , we denote a fractional derivative defined in the Caputo sense (see Definition 4 below). The left three terms in differential Eq. (1) may be identified as fractional diffusion (corresponding to Lévy-flight processes), advection (with velocity γ) and a chemical reaction term represented by f . For simplicity, the boundary conditions are taken to be of Dirichlet type. To define the fractional derivative we need first to set up the function space of possible solutions and to derive some useful properties (see also [15]):

Definition 1. A real function $g(x), x > 0$, lies in the function space C_γ , $\gamma \in \mathbb{R}$, if there exists a real number $p > \gamma$ such that g can be written as $g(x) = x^p g_1(x)$ with $g_1(x) \in C[0, \infty)$. It is clear that the property $C_{\gamma_1} \subset C_{\gamma_2}$ for $\gamma_2 \leq \gamma_1$ holds.

Definition 2. A function $g(x), x > 0$, lies in the function space C_γ^m , $m \in \mathbb{N} \cup \{0\}$, if $g^{(m)} \in C_\gamma$.

Definition 3. The left-sided Riemann–Liouville fractional integral \mathcal{J}^α of order $\alpha \geq 0$ of a function $g \in C_\gamma$, $\gamma \geq -1$ is defined as

$$\begin{cases} \mathcal{J}^\alpha g(x) = \frac{1}{\Gamma(\alpha)} \int_0^x \frac{g(t)}{(x-t)^{1-\alpha}} dt, & \alpha > 0, x > 0, \\ \mathcal{J}^0 g(x) = g(x), \end{cases} \quad (2)$$

where Γ denotes the Euler-gamma function that interpolates the factorial in integer values (with a shift of one unit): $\Gamma(m+1) = m!$, $m \in \mathbb{N}$.

Definition 4. Let $g \in C_{-1}^m$, $m \in \mathbb{N} \cup \{0\}$. Then the left-sided Caputo fractional derivative $\mathcal{D}_C^\alpha g$ is defined as

$$\mathcal{D}_C^\alpha g(x) = \mathcal{J}^{m-\alpha} g^{(m)}(x), \quad m-1 < \alpha \leq m, m \in \mathbb{N}. \quad (3)$$

The following properties for \mathcal{J}^α and \mathcal{D}_C^α can be derived [15]:

$$\begin{cases} \mathcal{J}^\alpha \mathcal{J}^\nu g(x) = \mathcal{J}^\nu \mathcal{J}^\alpha g(x) = \mathcal{J}^{\alpha+\nu} g(x), & \alpha, \nu \geq 0, g \in C_\gamma, \gamma \geq -1, \\ \mathcal{J}^\alpha x^\delta = \frac{\Gamma(\delta+1)}{\Gamma(\delta+\alpha+1)} x^{\delta+\alpha}, & \alpha > 0, \delta > -1, x > 0, \\ \mathcal{D}_C^\alpha \mathcal{J}^\alpha g(x) = g(x), \\ \mathcal{J}^\alpha \mathcal{D}_C^\alpha g(x) = g(x) - \sum_{k=0}^{m-1} g^{(k)}(0^+) \frac{x^k}{k!}, & m-1 < \alpha \leq m, x > 0, \\ \mathcal{D}_C^\alpha x^\delta = \frac{\Gamma(\delta+1)}{\Gamma(\delta-\alpha+1)} x^{\delta-\alpha}, & \alpha > 0, \delta > -1, x > 0, \end{cases} \quad (4)$$

where $g^{(k)}(0^+) := \lim_{x \downarrow 0} g^{(k)}(x)$. The first result shows the so-called semi-group property of fractional integrals. The second formula is a generalization of the integer counter-part: $\mathcal{J}^m x^k = \frac{k!}{(m+k)!} x^{k+m}$. The third and fourth properties indicate that \mathcal{J}^α and \mathcal{D}_C^α are not each other's inverses, unless a remainder term is zero. The fifth property is the derivative counterpart of the second one. This can be forced, however, by further restricting the function space C_γ^m . The consistency of the fractional derivative with respect to the traditional integer derivative can be expressed by the following result:

Lemma 1. The Caputo fractional derivative \mathcal{D}_C^α with $m-1 < \alpha \leq m$ is consistent with the integer-order derivative $\frac{d^m}{dx^m}$ for $m \in \mathbb{N}$.

Proof. For $g \in C^{m+1}([0, \infty))$, we write

$$\begin{aligned} \mathcal{D}_C^\alpha \{g\}(x) &= \frac{1}{\Gamma(m-\alpha)} \int_0^x \frac{g^{(m)}(s)}{(x-s)^{1-(m-\alpha)}} ds \\ &= \frac{1}{\Gamma(m-\alpha)} \left[-\frac{(x-s)^{m-\alpha}}{m-\alpha} g^{(m)}(s) \Big|_{s=0}^{s=x} + \int_0^x \frac{(x-s)^{m-\alpha}}{m-\alpha} g^{(m+1)}(s) ds \right] \\ &= \frac{1}{\Gamma(m-\alpha+1)} \left[0 + x^{m-\alpha} g^{(m)}(0) + \int_0^x (x-s)^{m-\alpha} g^{(m+1)}(s) ds \right] \end{aligned}$$

and taking the limit: $\alpha \in \mathbb{R} \rightarrow m \in \mathbb{N}$ with $m-1 \leq \alpha \leq m$ yields:

$$\begin{aligned}
 &= \frac{1}{\Gamma(1)} \left[g^{(m)}(0) + \int_0^x g^{(m+1)}(s) ds \right] \\
 &= g^{(m)}(0) + g^{(m)}(x) - g^{(m)}(0) = \frac{d^m g}{dx^m}(x).
 \end{aligned}$$

□

Note that the solution of boundary-value model (1) does not necessarily need to have a unique solution. It is known, for example, that for exponential-type functions g there may be zero, one or two solutions, depending on a parameter in the model (see [20,21]).

3. The homotopy perturbation method (HPM)

In this section, we describe a semi-analytical technique to approximate solutions of model (1). To explain the underlying concept of approximating solutions of the BV-problems (1), we first define a more general nonlinear differential equation by

$$D(u) = h(x), \quad x \in \Omega \subset \mathbb{R} \tag{5}$$

with boundary conditions

$$\mathcal{B}\left(u, \frac{\partial u}{\partial x}\right) = 0, \quad x \in \partial\Omega. \tag{6}$$

Here, D describes a differential operator, \mathcal{B} a boundary operator, h a given analytic function and $\partial\Omega$ the boundary of the spatial domain Ω , respectively. It is useful to divide the operator D into two parts which we denote by \mathcal{L} and \mathcal{N} , where \mathcal{L} is a linear operator and \mathcal{N} the remaining nonlinear part of the operator. Eq. (5) may then be written as

$$\mathcal{L}(u) + \mathcal{N}(u) = h(x). \tag{7}$$

We construct a homotopy $u(x; p) : \Omega \times [0, 1] \rightarrow \mathbb{R}$ which satisfies

$$\mathcal{H}(u; p) := (1 - p)[\mathcal{L}(u) - \mathcal{L}(v_0)] + p[D(u) - h(x)] = 0.$$

This is equivalent to

$$\mathcal{H}(u; p) = \mathcal{L}(u) - \mathcal{L}(v_0) + p\mathcal{L}(v_0) + p[\mathcal{N}(u) - h(x)] = 0. \tag{8}$$

In Eq. (8), $p \in [0, 1]$ represents a so-called embedding parameter, and v_0 can be viewed as an ‘initial’ approximation of the original model (5) which satisfies boundary condition (6). Obviously, from (7) and (8) it follows that

$$\begin{cases} \mathcal{H}(u; 0) = \mathcal{L}(u) - \mathcal{L}(v_0) = 0 \\ \mathcal{H}(u; 1) = D(u) - h(x) = 0. \end{cases} \tag{9}$$

The process of deforming p from zero to unity in (8) is just the deformation of $u(x; p)$ from the chosen function $u(x; 0) = v_0(x)$ to the solution $u(x; 1) = u(x)$ of differential Eq. (5). The term deformation stems from topology and the relation between the expressions $\mathcal{L}(u) - \mathcal{L}(v_0)$ and $D(u) - h(x)$ is called a homotopy. According to the homotopy perturbation method, the assumption is made that the solution of Eq. (8) can be written as a formal power series in the embedding parameter p :

$$u(x; p) = v_0(x) + v_1(x)p + v_2(x)p^2 + \dots = \sum_{k=0}^{\infty} v_k(x)p^k. \tag{10}$$

Finally, on setting $p = 1$, this results in the formal solution

$$u(x) = \lim_{p \rightarrow 1} u(x; p) = \sum_{k=1}^{\infty} v_k(x). \tag{11}$$

Approximations to $u(x)$ are obtained by truncating the infinite series to:

$$u(x) \approx V_N(x) := \sum_{k=1}^N v_k(x). \tag{12}$$

The described approximation technique is called the homotopy perturbation method (HPM). This method has the advantage that it overcomes the limitations of the traditional perturbation methods, in which the used parameter is assumed to be small. The convergence of series (10) depends on the nonlinear differential operator D . In general, the second derivative with respect to u of the nonlinear part \mathcal{N} in the splitting (7) must be sufficiently small, since the parameter p may be relatively large, in fact we take $p \rightarrow 1$. Furthermore, to ensure convergence of the series the following estimate [1] must hold: $\|\mathcal{L}^{-1} \frac{\partial \mathcal{N}}{\partial v}\| < 1$. For more details on the convergence of HPM we refer to [1,23]. It may be clear from the construction above that the choice of the homotopy is not unique and therefore, the convergence (or divergence) also depends on

that choice. Unfortunately, there exists no general theory yet to deal with this problem and each case has to be analyzed separately.

Next, we work out the described concept of HPM for boundary-value problem (1). For this model we take the homotopy defined by

$$\begin{cases} \epsilon \mathcal{D}_C^\alpha u + p[\gamma u' + f(u) - S(x)] = 0, & 1 < \alpha \leq 2, \\ u(0; p) = u_L, \quad u(1; p) = u_R, \quad p \in [0, 1]. \end{cases} \quad (13)$$

To obtain subsequent approximations for v_0, v_1, \dots , we use series (10), the linearity of the operator \mathcal{D}_C^α and a Taylor expansion of the function f around $u = 0$:

$$\begin{aligned} f(u) &= f(0) + f'(0)u + f''(0)\frac{u^2}{2!} + \dots \\ &= f'(0)v_0 + \frac{f''(0)}{2}v_0^2 + \frac{f'''(0)}{6}v_0^3 + \dots \\ &\quad + p\left[f'(0)v_1 + v_0v_1f''(0) + \frac{5}{12}v_0^2v_1f'''(0) + \dots\right] \\ &\quad + p^2\left[f'(0)v_2 + (2v_0v_2 + v_1^2)\frac{f''(0)}{2} + \left(\frac{5}{2}v_0^2v_2 + 3v_0v_1^2\right)\frac{f'''(0)}{6} + \dots\right] \\ &\quad + p^3\left[f'(0)v_3 + (v_0v_3 + v_1v_2)f''(0) + \left(\frac{5}{2}v_0^2v_3 + 6v_0v_1v_2 + v_1^3\right)\frac{f'''(0)}{6} + \dots\right] \\ &\quad + \mathcal{O}(p^4). \end{aligned} \quad (14)$$

Note that this expansion can also be derived by applying the theory of Schur polynomials as described in [24]. Substituting (14) and (10) into (13) and collecting terms of equal power in the homotopy parameter p , we obtain

$$\begin{cases} p^0: \quad \epsilon \mathcal{D}_C^\alpha v_0 = 0, \\ v_0(0) = u_L, \quad v_0(1) = u_R \quad \Rightarrow v_0(x) = u_L + (u_R - u_L)x \end{cases} \quad (15)$$

$$\begin{cases} p^1: \quad \epsilon \mathcal{D}_C^\alpha v_1 + \gamma v_1' + v_0f'(0) + \frac{1}{2}v_0^2f''(0) + \frac{1}{6}v_0^3f'''(0) + \dots - S(x) = 0, \\ v_1(0) = 0, \quad v_1(1) = 0 \quad \Rightarrow v_1(x) = \dots \end{cases} \quad (16)$$

$$\begin{cases} p^2: \quad \epsilon \mathcal{D}_C^\alpha v_2 + \gamma v_2' + v_1f'(0) + v_0v_1f''(0) + \frac{5}{12}v_0^2v_1f'''(0) + \dots = 0, \\ v_2(0) = 0, \quad v_2(1) = 0 \quad \Rightarrow v_2(x) = \dots \end{cases} \quad (17)$$

$$\begin{cases} p^3: \quad \epsilon \mathcal{D}_C^\alpha v_3 + \gamma v_3' + v_2f'(0) + \frac{1}{2}(2v_0v_2 + v_1^2)f''(0) \\ \quad \quad \quad + \frac{1}{6}\left(\frac{5}{2}v_0^2v_2 + 3v_0v_1^2\right)f'''(0) + \dots = 0, \\ v_3(0) = 0, \quad v_3(1) = 0 \quad \Rightarrow v_3(x) = \dots \end{cases} \quad (18)$$

$$\begin{cases} p^4: \quad \epsilon \mathcal{D}_C^\alpha v_4 + \gamma v_4' + v_3f'(0) + (v_0v_3 + v_1v_2)f''(0) \\ \quad \quad \quad + \frac{1}{6}\left(\frac{5}{2}v_0^2v_3 + 6v_0v_1v_2 + v_1^3\right)f'''(0) + \dots = 0, \\ v_4(0) = 0, \quad v_4(1) = 0 \quad \Rightarrow v_4(x) = \dots, \textit{ etcetera}. \end{cases} \quad (19)$$

In each step, we apply a fractional integral (see Eqs. (2) and (4)) to obtain the intermediate solutions $V_0(x), V_1(x), \dots, V_N(x)$. The first nonlinear term in (14) is u^2 and yields

$$\begin{aligned} u^2 &= \left(\sum_{n=0}^{\infty} v_n p^n\right) \left(\sum_{k=0}^{\infty} v_k p^k\right), \\ &= \sum_{n=0}^{\infty} \left[\sum_{i=0}^n v_i p^i v_{n-i} p^{n-i} \right], \\ &= \sum_{n=0}^{\infty} \left[\sum_{i=0}^n v_i v_{n-i} p^n \right] = \sum_{n=0}^{\infty} \left[\sum_{i=0}^n v_i v_{n-i} \right] p^n := \sum_{n=0}^{\infty} w_n^{(2)} p^n. \end{aligned} \quad (20)$$

where $w_n^{(2)}$ is a weight-function depending on products of the coefficients v_n . For the term with u^3 in (14) we set

$$\begin{aligned}
 u^3 &= \sum_{n=0}^{\infty} \left[\sum_{i=0}^n v_i v_{n-i} p^n \right] \left(\sum_{k=0}^{\infty} v_k p^k \right), \\
 &= \sum_{n=0}^{\infty} \left[\sum_{i=0}^n \left(\sum_{j=0}^i v_j v_{i-j} \right) p^i v_{n-i} p^{n-i} \right], \\
 &= \sum_{n=0}^{\infty} \left[\sum_{i=0}^n \left(\sum_{j=0}^i v_j v_{i-j} \right) v_{n-i} \right] p^n := \sum_{n=0}^{\infty} w_n^{(3)} p^n,
 \end{aligned} \tag{21}$$

and following similar steps for higher powers of u we can write

$$u^n = \sum_{r=0}^{\infty} w_n^{(r)} p^r, \tag{22}$$

where

$$w_n^{(r)} = \sum_{i=0}^n \left[\sum_{j_1=0}^i \left(\sum_{j_2=0}^{j_1} \dots \left(\sum_{j_{r-2}=0}^{j_{r-1}} v_{j_{r-1}} v_{j_{r-1}-j_{r-2}} \dots \right) \right) \right] v_{n-i}.$$

Next, we substitute these expressions into Eq. (14):

$$\begin{aligned}
 f(u) &= f(0) + f'(0) \sum_{n=0}^{\infty} v_n p^n + f''(0) \frac{\sum_{n=0}^{\infty} w_n^{(2)} p^n}{2!} + f'''(0) \frac{\sum_{n=0}^{\infty} w_n^{(3)} p^n}{3!} + \dots \\
 &= \sum_{m=0}^{\infty} \left[\frac{f^{(m)}(0)}{m!} \sum_{n=0}^{\infty} w_n^{(m)} p^n \right].
 \end{aligned} \tag{23}$$

Eq. (23) is a general formula which enables us to calculate the step solutions v_k in HPM. To our knowledge, this the first time such a general expression for the HPM solutions v_k is explicitly written out.

4. Theoretical results

4.1. A comparison between HPM and the Adomian decomposition method

In this section, we first present another semi-analytical method: the Adomian Decomposition Method (ADM) (see [5,25,26,27]). Although this method provides us a series solution from a different perspective, it has a strong relation with the final HPM series. This is stated in the following lemma:

Lemma 2. For boundary-value models of type (5) the series methods HPM and ADM yield equivalent expansions.

Proof. We consider again the nonlinear BV-model (5). According to ADM, we write $u(x) = v_0(x) + \sum_{n=1}^{\infty} v_n(x)$. Here $u_0(x) = \mathcal{L}^{-1}[h(x)]$ and $u_n(x) = -\mathcal{L}^{-1}[A_{n-1}(x)]$, in which \mathcal{L}^{-1} is the inverse operator of \mathcal{L}^{-1} and $A_n(x)$ are the so-called Adomian polynomials

$$A_n(x) = \frac{1}{n!} \left[\frac{\partial^n}{\partial p^n} \mathcal{N} \left(v_0(x) + \sum_{n=1}^{\infty} v_n(x) p^n \right) \right] \Big|_{p=0}. \tag{24}$$

On the other hand, the general HPM formula is as follows:

$$(1 - p)\mathcal{L}[u(x; p) - v_0(x)] = -p\mathcal{N}[u(x; p) - h(x)], \tag{25}$$

where $u(x; p)$ is a unknown dependent variable. It clearly holds $u(x; 0) = v_0(x)$ and $u(x; 1) = u(x)$. Then we expand $u(x; p)$ in a power series of p :

$$u(x; p) = v_0(x) + \sum_{n=1}^{\infty} v_n(x) p^n, \quad \text{and} \quad V_n(x) = \frac{1}{n!} \frac{\partial^n u(x; p)}{\partial p^n} \Big|_{p=0}. \tag{26}$$

Note that we have a great freedom to choose the initial approximation in HPM. First, we substitute $p = 1$ in (10):

$$u(x) = v_0(x) + \sum_{n=1}^{\infty} v_n(x), \tag{27}$$

which becomes the same in ADM. Then, we differentiate (25) n times with respect to p , divide by $n!$ and finally set $p = 0$:

$$\mathcal{L}[v_1(x)] = -\mathcal{N}[v_0(x)] - h(x) \quad \text{when } n = 1, \quad \text{and} \tag{28}$$

$$\mathcal{L}[v_n(x) - v_{n-1}(x)] = -\frac{1}{(n-1)!} \left. \frac{\partial^n \mathcal{N}[u(x; p)]}{\partial p^n} \right|_{p=0}, \quad \text{when } n \geq 1. \tag{29}$$

As we have mentioned before, we have a great freedom to choose the auxiliary linear operator and the initial guess. Then we can choose:

$$\mathcal{L} = \mathcal{L}_0, \quad v_0(x) = \mathcal{L}_0^{-1}[g(x)]. \tag{30}$$

We reorganize (28) and (29) to obtain:

$$\mathcal{L}_0[v_1(x)] = h(x) - \mathcal{L}_0[v_0(x)] - \mathcal{N}_0[v_0(x)], \tag{31}$$

and

$$\mathcal{L}_0[v_n(x)] = \mathcal{L}_0[v_{n-1}(x)] - \frac{1}{(n-1)!} \left. \frac{\partial^n \mathcal{L}_0[u(x; p)]}{\partial p^n} \right|_{p=0} - \frac{1}{(n-1)!} \left. \frac{\partial^n \mathcal{N}_0[u(x; p)]}{\partial p^n} \right|_{p=0}. \tag{32}$$

We recognize that

$$h(x) - \mathcal{L}_0[v_0(x)] = 0, \tag{33}$$

from which it follows that

$$\mathcal{L}_0[v_1(x)] = -A_0(x), \tag{34}$$

according to the definition of Adomian polynomials. Making use of (26), it holds

$$\begin{aligned} &\mathcal{L}_0[v_{n-1}(x)] - \frac{1}{(n-1)!} \left. \frac{\partial^n \mathcal{L}_0[u(x; p)]}{\partial p^n} \right|_{p=0} \\ &= \mathcal{L}_0[v_{n-1}(x)] - \mathcal{L}_0 \left[\frac{1}{(n-1)!} \left. \frac{\partial^n [u(x; p)]}{\partial p^n} \right|_{p=0} \right] \\ &= \mathcal{L}_0[v_{n-1}(x)] - \mathcal{L}_0[v_{n-1}(x)] \\ &= 0. \end{aligned} \tag{35}$$

Thus, Eq. (32) becomes

$$\mathcal{L}_0[v_n(x)] = -\frac{1}{(n-1)!} \left. \frac{\partial^n \mathcal{N}_0[u(x; p)]}{\partial p^n} \right|_{p=0}. \tag{36}$$

We substitute (26) into the above expression, it becomes according to the definition of Adomian polynomials

$$\begin{aligned} \mathcal{L}_0[v_n(x)] &= -\frac{1}{(n-1)!} \left[\left. \frac{\partial^n}{\partial p^n} \mathcal{N}_0 \left(v_0(x) + \sum_{n=1}^{\infty} v_n(x) p^n \right) \right|_{p=0} \right] \\ &= -A_{n-1}(x), \end{aligned} \tag{37}$$

which proves that ADM is equivalent with HPM. □

4.2. Convergence of HPM

Analyzing the convergence of series (11) in HPM is not trivial. It highly depends on the parameters in the underlying model. In some cases it even diverges. In the case of a convergent series, it can be shown to converge very fast to the exact solution of the nonlinear model. We will give an example to show the potentially fast convergence of HPM.

Example 1 (“Spectral” convergence of HPM).

$$\begin{cases} u'' + u = g(x), \\ u(0) = u(1) = 0. \end{cases} \tag{38}$$

The exact solution reads for a given $g(x)$:

$$u^*(x) = \sum_{n=1}^{\infty} b_n \sin(n\pi x) \quad \text{with} \quad b_n = 2 \int_0^1 u^*(x) \sin(n\pi x) dx \tag{39}$$

and we take

$$g(x) = \sum_{n=1}^{\infty} (1 - n^2\pi^2) b_n \sin(n\pi x). \tag{40}$$

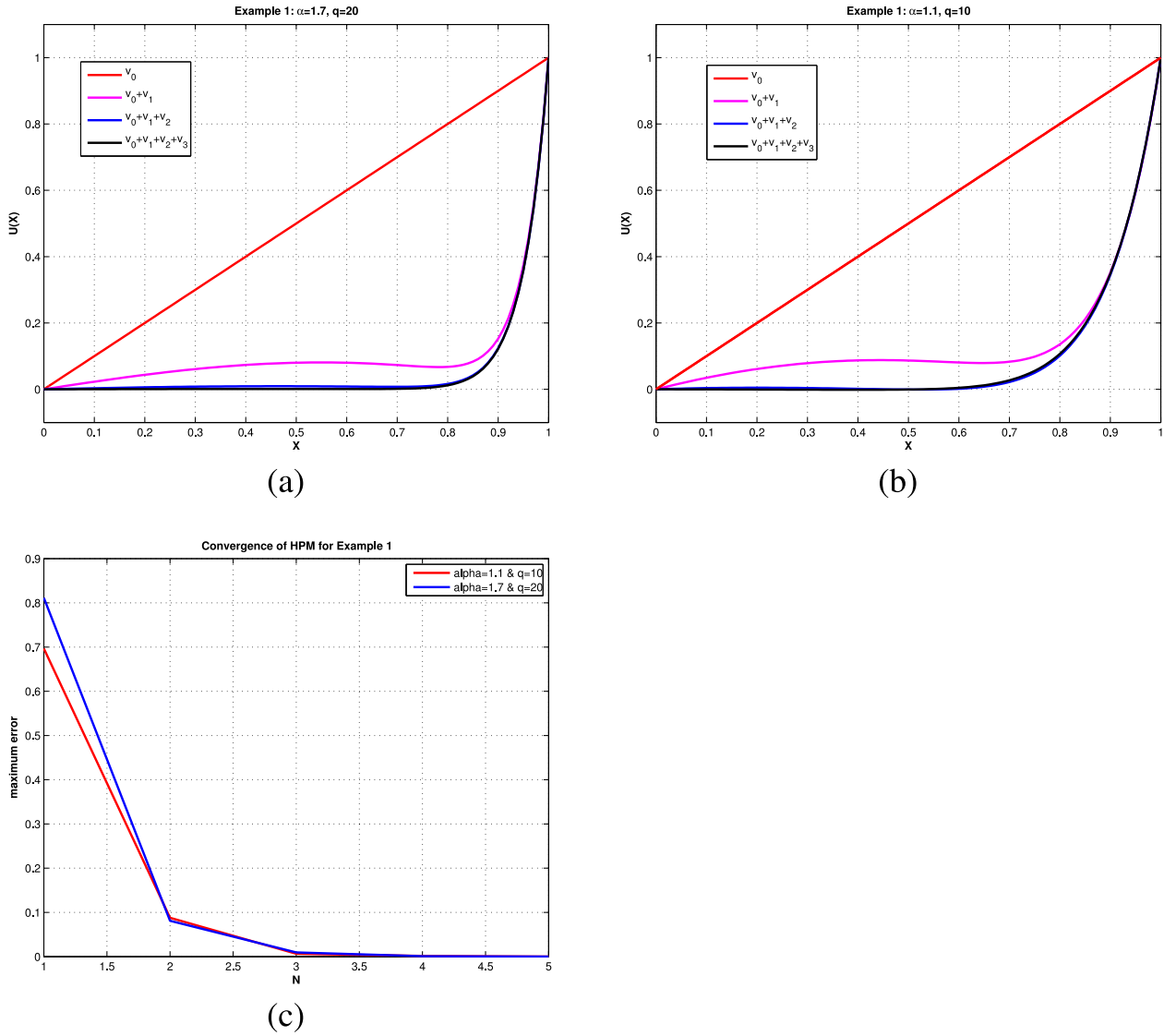


Fig. 1. Panels (a) and (b) show HPM solutions as a function of the index N for different values of the fractional order α and the power q in model (49). Panel (c) displays the fast convergence of HPM for the two cases.

Suppose that the exact solution u^* is bounded: $\|u^*\|_2 = M < \infty$. Then it follows that:

$$|b_n| \leq 2 \int_0^1 |u^*(x)| |\sin(n\pi x)| dx = 2 \int_0^1 |u^*(x)| dx \tag{41}$$

$$\leq 2 \|u^*\|_2 \|1\|_2 = 2 \|u^*\| = 2M. \tag{42}$$

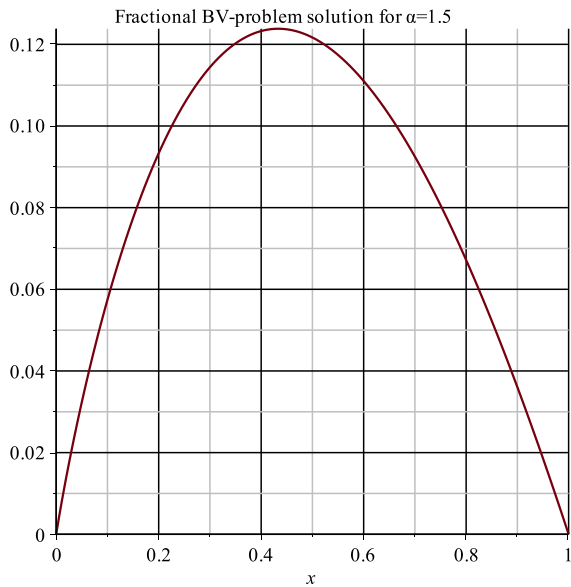
The HPM solution is obtained in the way as described in Section 3. First, we write the homotopy:

$$\begin{cases} u'' + p(u - g(x)) = 0, \\ u(0) = u(1) = 0. \end{cases} \tag{43}$$

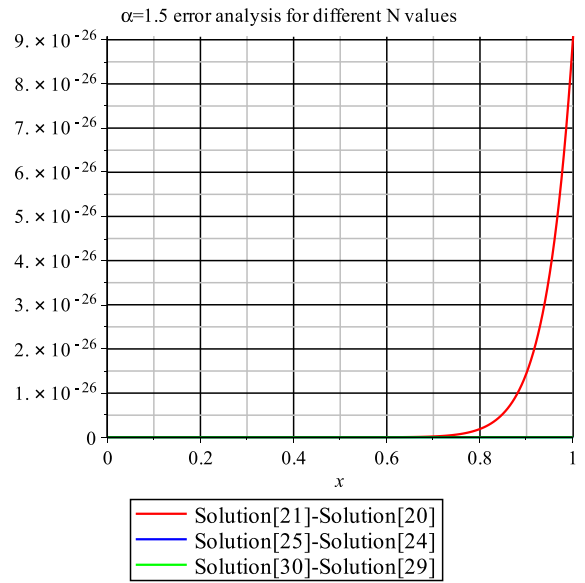
Then we select the equations for equal powers of p :

$$p^0 : \begin{cases} (v_0)'' = 0, \\ v_0(0) = 0, v_0(1) = 0 \end{cases} \Rightarrow v_0(x) = 0. \tag{44}$$

$$p^1 : \begin{cases} (v_1)'' + v_0 = h(x), \\ v_1(0) = 0, v_1(1) = 0 \end{cases} \Rightarrow v_1(x) = \sum_{n=1}^{\infty} \left(1 - \frac{1}{n^2\pi^2}\right) b_n \sin(n\pi x). \tag{45}$$

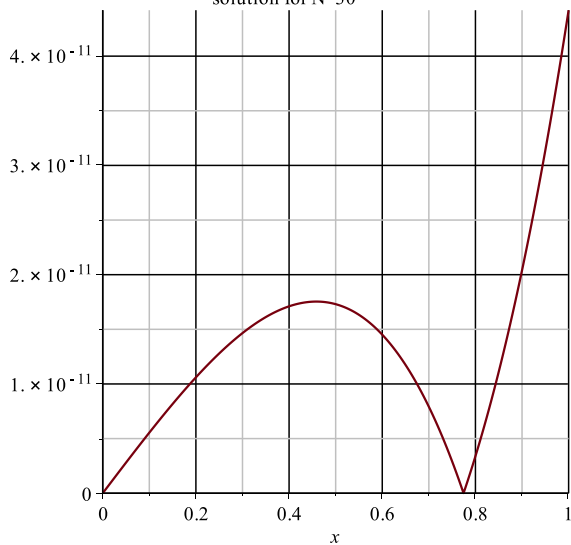


(a)



(b)

Fractional BV-problem error analysis between HPM solution and exact solution for N=30



(c)

Fig. 2. HPM solutions for example 3 for $\alpha = 1.5$ (upper two plots) and the error for $N=30$ and $\alpha = 2$ (lower plot).

$$p^2 : \begin{cases} (v_2)'' + v_1 = 0, \\ v_2(0) = 0, v_2(1) = 0 \end{cases} \Rightarrow v_2(x) = \sum_{n=1}^{\infty} \left(\frac{1}{n^2\pi^2} - \frac{1}{n^4\pi^4} \right) b_n \sin(n\pi x). \tag{46}$$

$$p^3 : \begin{cases} (v_3)'' + v_2 = 0, \\ v_3(0) = 0, v_3(1) = 0 \end{cases} \Rightarrow v_3(x) = \sum_{n=1}^{\infty} \left(\frac{1}{n^4\pi^4} - \frac{1}{n^6\pi^6} \right) b_n \sin(n\pi x). \tag{47}$$

The HPM solution becomes: $u(x) = \sum_{k=1}^{\infty} v_k(x) = \lim_{N \rightarrow \infty} V_N(x)$

$$= \lim_{N \rightarrow \infty} \sum_{n=1}^{\infty} \left(1 - \frac{1}{(n\pi)^{2N}} \right) b_n \sin(n\pi x).$$

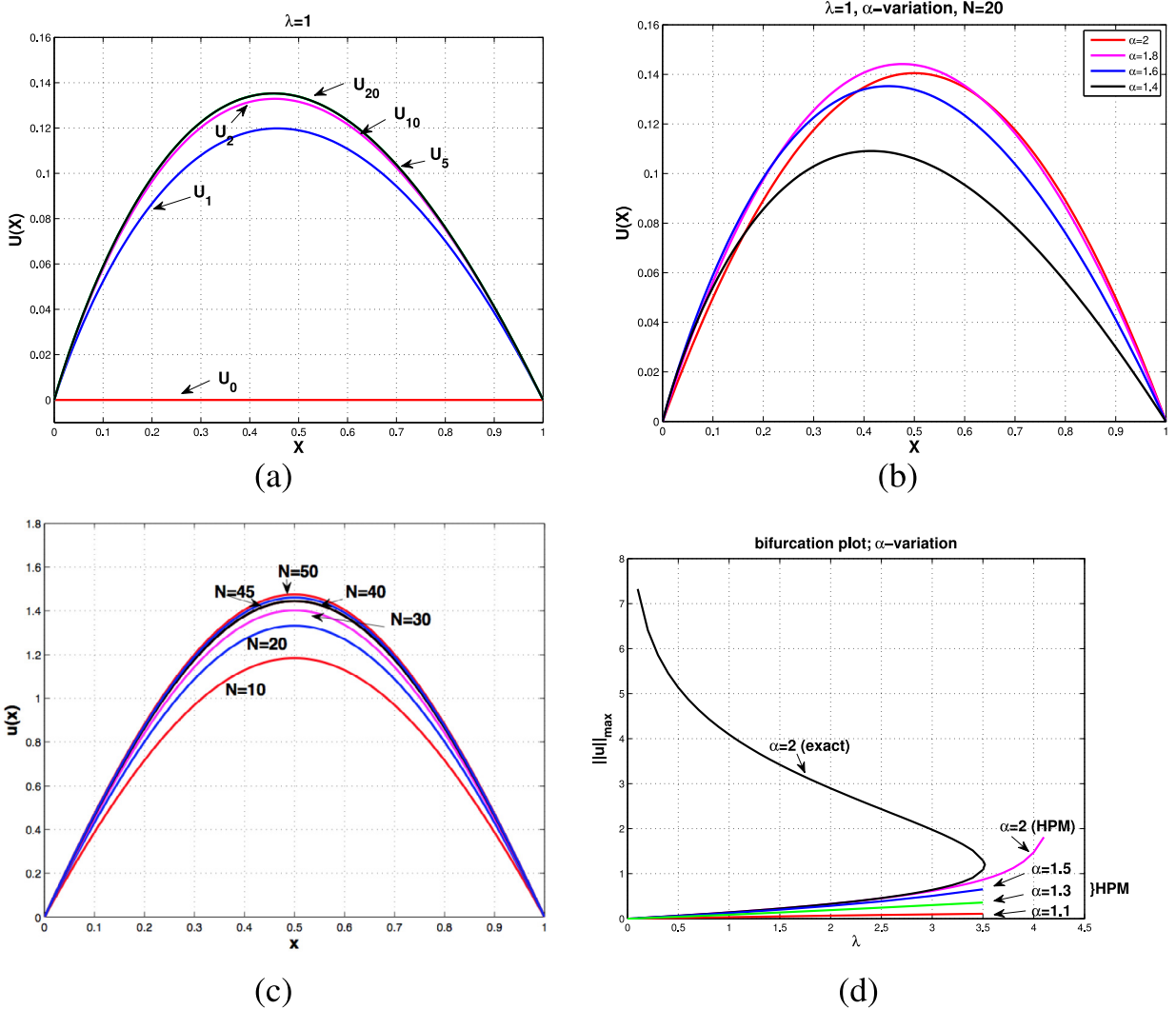


Fig. 3. Numerical results for the Gelfand–Bratu model defined by Eq. (58). In panel (c), we can see that the HPM solution is converging for $\lambda = 4$ and $\alpha = 2$.

We can now easily find an estimate for the error as a function of N :

$$\begin{aligned}
 e_N(x) &:= u^*(x) - V_N(x), \\
 &= \sum_{n=1}^{\infty} \frac{1}{(n\pi)^{2N}} b_n \sin(n\pi x),
 \end{aligned}$$

which gives

$$\begin{aligned}
 \|e_N\|_2 &= \left\| \sum_{n=1}^{\infty} \left(\frac{1}{(n\pi)^{2N}} \right) b_n \sin(n\pi x) \right\|_2, \\
 &\leq \sum_{n=1}^{\infty} \frac{|b_n|}{(n\pi)^{2N}}, \\
 &\leq \sum_{n=1}^{\infty} \frac{2M}{(n\pi)^{2N}}, \\
 &\leq \frac{2M}{\pi^{2N}} \sum_{n=1}^{\infty} \frac{1}{n^2} \\
 &= \frac{M}{3\pi^{2N-2}}.
 \end{aligned}$$

Table 1
Maximum HPM error for $q = 10$ and for $q = 20$.

N	$\alpha = 1.1$	$\alpha = 1.7$
1	0.08582180	0.07493868
2	0.00486217	0.00851444
3	0.00158691	0.00089426
4	0.00013589	0.00009150
5	0.00002649	0.00000935
N	$\alpha = 1.1$	$\alpha = 1.7$
1	0.10386288	0.08023764
2	0.00696762	0.00930574
3	0.00171177	0.00098390
4	0.00017720	0.00010091
5	0.00002596	0.00001031

This example shows, at least for this specific example, 'spectral' convergence of the HPM approximations. In general, this is not necessarily the case, of course. The HPM series solution can converge (slowly, fast) or even diverge, depending on the situation. For this, we refer to [23,28,29] in which more general convergence results for HPM are discussed.

5. Numerical examples

In this section, we present numerical experiments to show the different aspects of HPM when applied to models of type (1).

5.1. Example 2: a linear fractional BV-model with a source term

First, we consider:

$$\begin{cases} \mathcal{D}_C^\alpha u + u = x^q + \frac{\Gamma(q+1)}{\Gamma(q-\alpha+1)} x^{q-\alpha}, & q > \alpha, \\ u(0) = 0, \quad u(1) = 1, \end{cases} \quad (49)$$

with the exact solution given by $u(x) = x^q$. We show the numerical HPM solutions for the cases $q = 10$ ($\alpha = 1.1$ and $\alpha = 1.7$) and $q = 20$ ($\alpha = 1.1$ and $\alpha = 1.7$) in Table 1. This table shows the effects of α and q values on the HPM solution. We observe that the lower α values and higher q values give higher maximum absolute errors. This example also demonstrates the fast convergence of HPM for linear fractional differential equations. In Fig. 1, we present the effect of different α values on the HPM solution. It is clear that the quality of HPM approximation is directly related to the fractional order α and the power q in the solution.

5.2. Example 3: an explicit HPM-solution

In this example, we study a linear fractional boundary-value model:

$$\begin{cases} \mathcal{D}_C^\alpha u + 1 + u = 0, & 1 < \alpha \leq 2, \\ u(0) = 0, \quad u(1) = 1. \end{cases} \quad (50)$$

For $\alpha = 2$ the exact solution reads $u(x) = \frac{1-\cos(1)}{\sin(1)} \sin(x) + \cos(x) - 1$. The lower figure in Fig. 2 depicts the error for $N = 30$ of the HPM solution for $\alpha = 2$. The upper plots in Fig. 2 illustrate the HPM solution for $N = 30$ (left plot) and the difference between two succeeding HPM solutions (right plot).

For this model, we can derive an explicit formula for the series solution. Following the HPM steps in Section 3, we separate the fractional derivative part and then multiply the remaining part with the parameter p :

$$\mathcal{D}_C^\alpha u = -p(1 + u) \quad (51)$$

Then we substitute assumption (10) into equation (51):

$$\mathcal{D}_C^\alpha (v_0 + pv_1 + p^2v_2 + p^3v_3 + \dots) = -p(1 + v_0 + pv_1 + p^2v_2 + \dots). \quad (52)$$

Collecting the equations for increasing powers of the parameter p , i.e. for $p^0, p^1, p^2, p^3, \dots$; we find:

$$p^0: \mathcal{D}_C^\alpha v_0 = 0 \Rightarrow \begin{cases} v_0(x) - v_0'(0)x = c_0 & v_0'(0) = \beta_0 \\ v_0(x) = \beta_0 x + c_0 \\ v_0(0) = v_0(1) = 0 & \Rightarrow \beta_0 = 0, \quad c_0 = 0 \\ v_0(x) = 0. \end{cases} \quad (53)$$

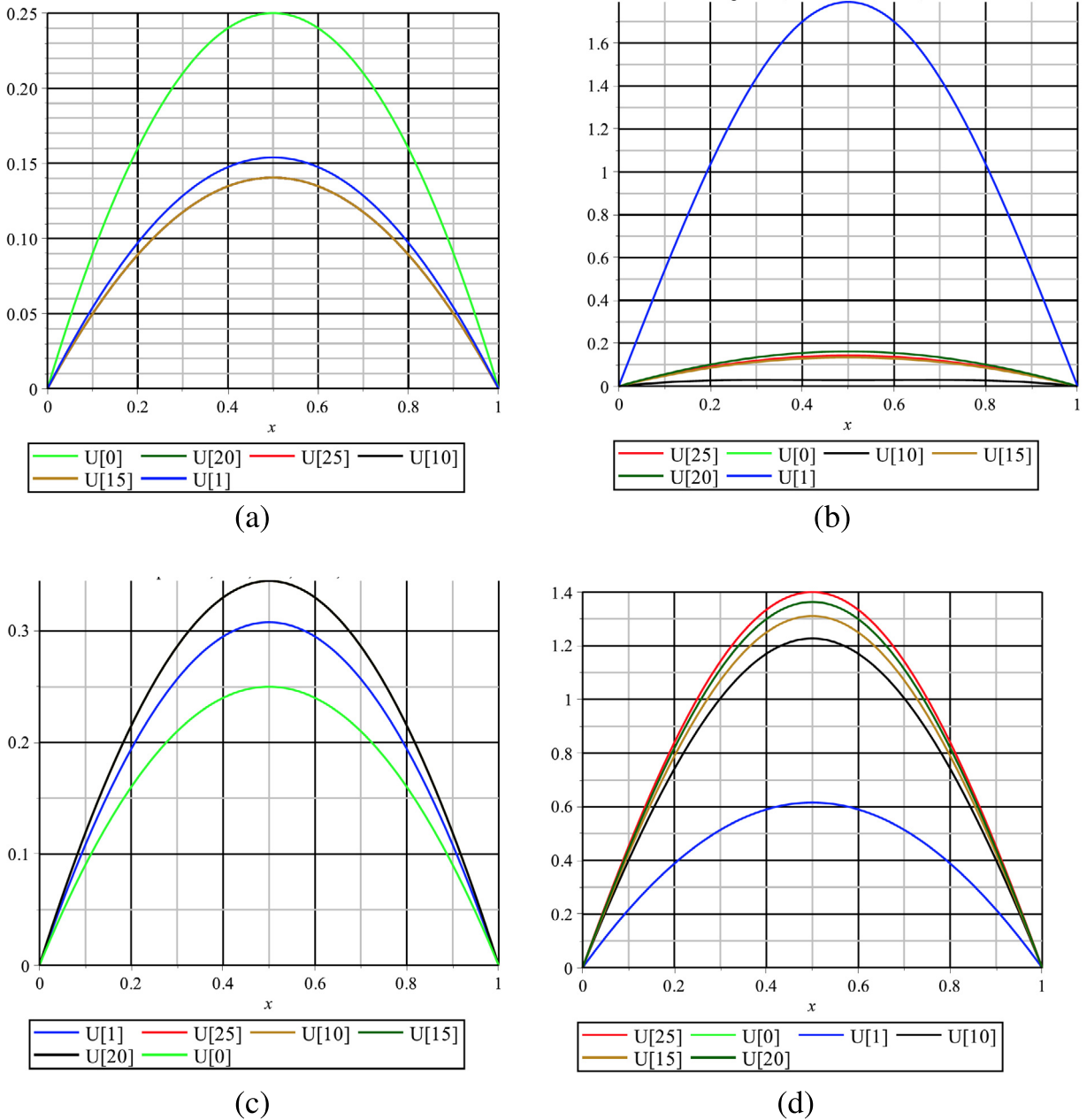


Fig. 4. Influence on the convergence of HPM depending on the parameters μ and A in model (58). Panel (a) shows the HPM solution solutions for $A = 1$ and $\lambda = 1$, panel (b) shows for $A = 20$ and $\lambda = 1$, panel (c) shows for $A = 5$ and $\lambda = 2$ and finally panel (d) shows the results for $A = 1$ and $\lambda = 4$.

$$p^1 : \mathcal{D}_c^\alpha v_1 = -1 - v_0 \Rightarrow \begin{cases} v_1(x) - v_1'(0)x = \frac{\Gamma(1)}{\Gamma(\alpha+1)}x^\alpha, \\ v_1(x) = -\frac{\beta_1}{\Gamma(\alpha+1)}x^\alpha + \beta_1x, \\ v_1(1) = 0 \Rightarrow \beta_1 = \frac{\Gamma(1)}{\Gamma(\alpha+1)}. \end{cases} \quad (54)$$

$$p^2 : \mathcal{D}_c^\alpha v_2 = -v_1 = \frac{\Gamma(1)}{\Gamma(\alpha+1)}x^\alpha - \beta_1x \Rightarrow \begin{cases} v_2(x) - v_2'(0)x = \mathcal{J}_c^\alpha \left[\frac{\Gamma(1)}{\Gamma(\alpha+1)}x^\alpha - \beta_1x \right], \\ v_2(x) = \frac{\beta_2}{\Gamma(2\alpha+1)}x^{2\alpha} - \beta_1 \frac{\Gamma(2)}{\Gamma(\alpha+2)}x^{\alpha+1} + \beta_2x, \\ v_2(1) = 0 \Rightarrow \beta_2 = \frac{\Gamma(1)}{\Gamma(2\alpha+1)} - \beta_1 \frac{\Gamma(2)}{\Gamma(\alpha+2)}. \end{cases} \quad (55)$$

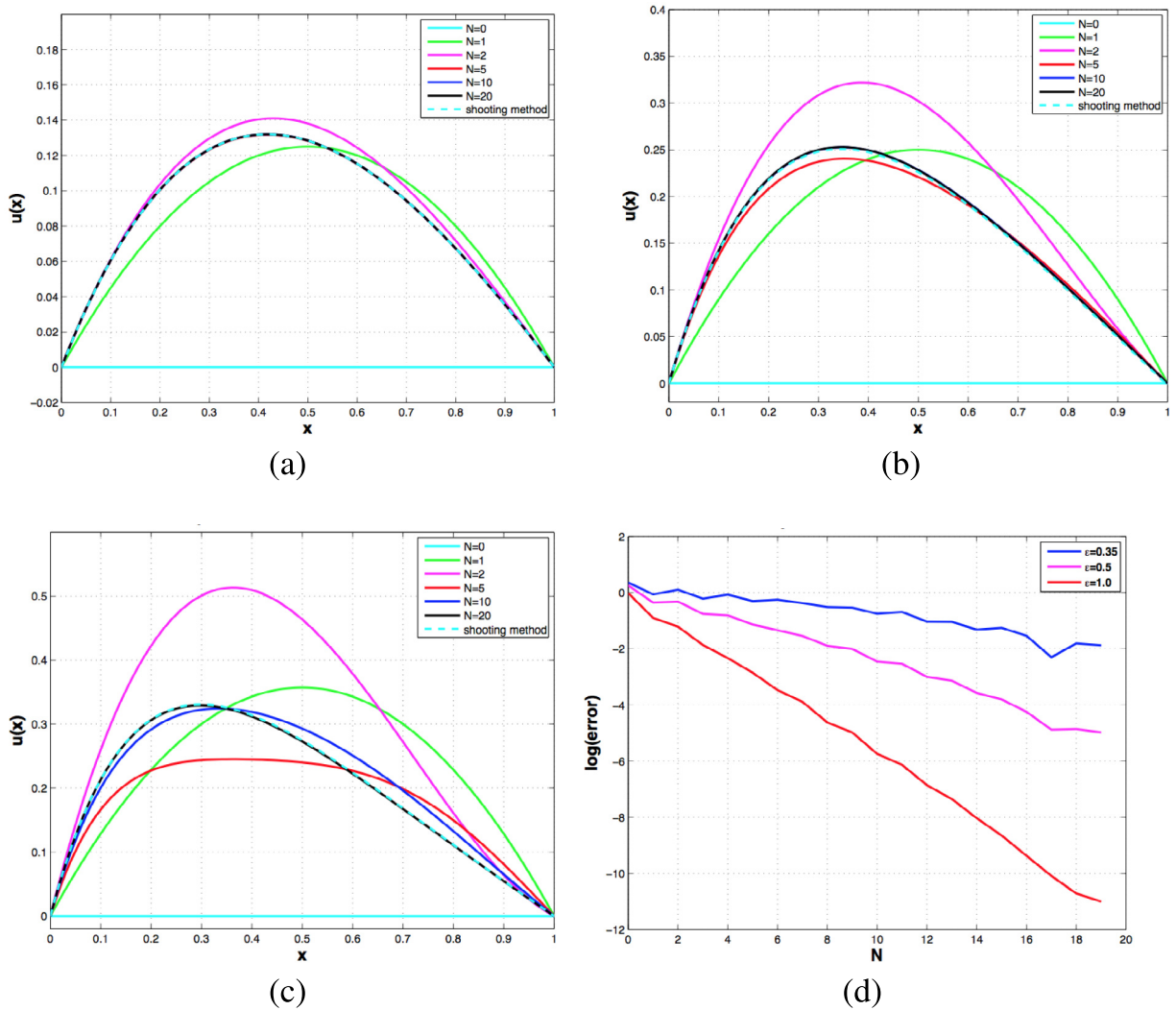


Fig. 5. Numerical results for the fractional Gelfand–Bratu model with damping (59): HPM solutions for $\epsilon = 1.0$ (a), $\epsilon = 0.5$ (b), $\epsilon = 0.35$ (c), and the error in the maximum norm as a function of the number of terms N in the approximation, respectively.

$$\begin{aligned}
 p^3 : \mathcal{D}_c^\alpha v_3 &= -v_2 = -\frac{\Gamma(1)}{\Gamma(2\alpha+1)}x^{2\alpha} + \beta_1 \frac{\Gamma(2)}{\Gamma(\alpha+2)}x^{\alpha+1} - \beta_2 x, \\
 \Rightarrow \begin{cases} v_3(x) - \underbrace{v_3'(0)}_{\beta_3} x &= \mathcal{J}_c^\alpha \left[-\frac{\Gamma(1)}{\Gamma(2\alpha+1)}x^{2\alpha} + \beta_1 \frac{\Gamma(2)}{\Gamma(\alpha+2)}x^{\alpha+1} - \beta_2 x \right], \\ v_3(x) &= -\frac{\Gamma(1)}{\Gamma(3\alpha+1)}x^{3\alpha} + \beta_1 \frac{\Gamma(2)}{\Gamma(\alpha+2)} \frac{\Gamma(\alpha+2)}{\Gamma(2\alpha+2)}x^{2\alpha+1} - \beta_2 \frac{\Gamma(2)}{\Gamma(\alpha+2)}x^{\alpha+1} + \beta_3, \\ v_3(1) = 0 &\Rightarrow \beta_3 = \frac{\Gamma(1)}{\Gamma(3\alpha+1)} - \beta_1 \frac{\Gamma(2)}{\Gamma(\alpha+2)} \frac{\Gamma(\alpha+2)}{\Gamma(2\alpha+2)} + \beta_2 \frac{\Gamma(2)}{\Gamma(\alpha+2)}. \end{cases} \tag{56}
 \end{aligned}$$

With induction we can generate the formula:

$$\begin{aligned}
 v_n(x) &= (-1)^n \frac{\Gamma(1)}{\Gamma(1+n\alpha)}x^{n\alpha} + \left[\sum_{k=1}^{n-1} (-1)^{k+1} \beta_k \left(\prod_{i=1}^{n-k} \frac{\Gamma(2+\alpha(i-1))}{\Gamma(2+i\alpha)} \right) x^{\alpha(n-k)+1} \right] + \beta_n x, \\
 \beta_n &= (-1)^{n+1} \frac{\Gamma(1)}{\Gamma(1+n\alpha)} + \left[\sum_{k=1}^{n-1} (-1)^k \beta_k \left(\prod_{i=1}^{n-k} \frac{\Gamma(2+\alpha(i-1))}{\Gamma(2+i\alpha)} \right) \right]. \tag{57}
 \end{aligned}$$

and finally we set $u(x) = u(x; 1) = \sum_{n=1}^\infty v_n(x)$.

This generated formula could provide us with higher-order HPM solutions. However, from a practical point of view, the use of formula (57) is not very efficient. Instead, it could serve for theoretical considerations.

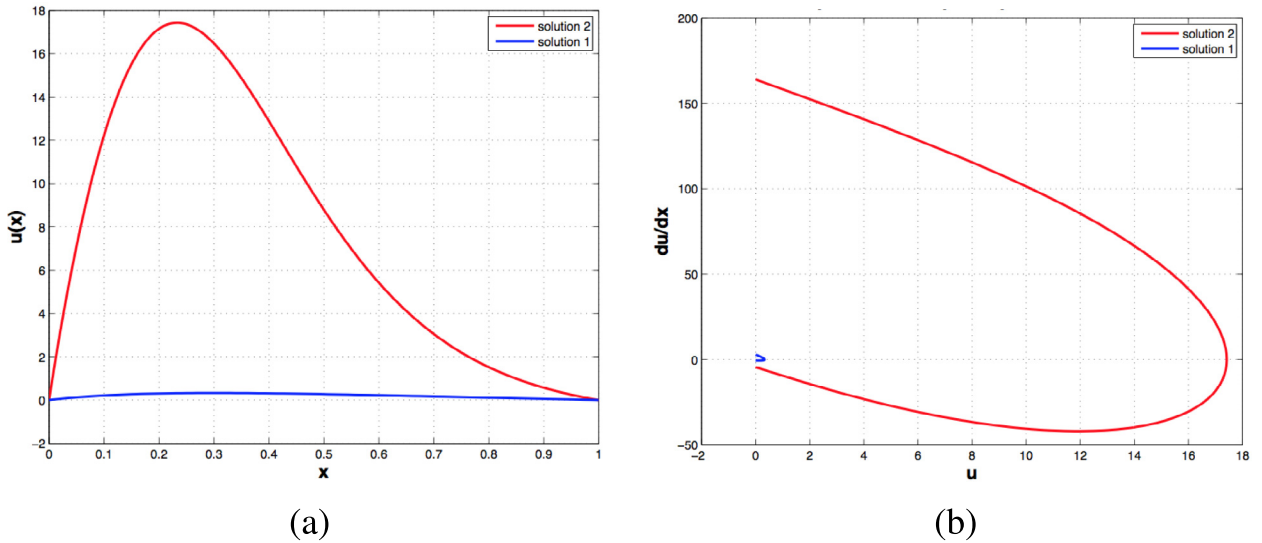


Fig. 6. Two different solutions in the fractional Gelfand–Bratu model with damping (59) for $\epsilon = 0.35$: in panel (a) these are displayed as a function of x and in panel (b) in the phase plan $(u, du/dx)$. These solutions were obtained by a shooting method and the existence is confirmed by analysis in [20]. Only the lower solution 1, shown in blue, can be detected by HPM.

Table 2
Errors in example 4 for $A = 1, \mu = 1$ and $\alpha = 2$.

N	Maximum error	Ratio test
1	0.09609375	0.384375
2	0.01230238	0.128025
3	0.00109586	0.089077
4	0.00002895	0.026416
5	0.00001244	0.429618
6	0.00000295	0.237384
...
10	$1.51651970 \cdot 10^{-9}$	0.236744
11	$1.72137047 \cdot 10^{-10}$	0.113508
12	$4.68366748 \cdot 10^{-13}$	0.001146

Table 3
Errors in example 4 for $A = 5, \mu = 1$ and $\alpha = 2$.

N	Maximum error	Ratio test
1	0.92317708	0.477083
2	0.20311499	0.445347
3	0.00370464	0.298901
4	0.01602912	0.061214
5	0.00548413	2.595368
6	0.00009242	0.753362
...
23	$1.72124479 \cdot 10^{-10}$	0.077870
24	$1.64598188 \cdot 10^{-10}$	3.667836
25	$9.76579753 \cdot 10^{-11}$	0.894541

5.3. Example 4: a fractional Gelfand–Bratu model

The following example is the fractional Gelfand–Bratu model with parameter μ :

$$\begin{cases} \mathcal{D}_C^\alpha u + \mu e^u = 0, \mu > 0, 1 < \alpha \leq 2, \\ u(0) = u(1) = 0. \end{cases} \tag{58}$$

In this model, we expand the nonlinear term e^u into a Taylor series to apply the fractional integral formulas in Eqs. (15)–(19) more efficiently. Note that for $\alpha = 2$, there may be zero, one or two solutions for this model, depending on the value of μ [22]. We use here the initial HPM approximation $u(x) = A x(1 - x)$ with $A \in \mathbb{R}$, which satisfies the boundary conditions. The effect of changing μ and A values on the HPM solution is presented in Tables 2–4. These tables show us that for higher μ and A values we need more steps to get a reasonable accuracy for $\alpha = 2$. We also included a ‘ratio test’ between differences

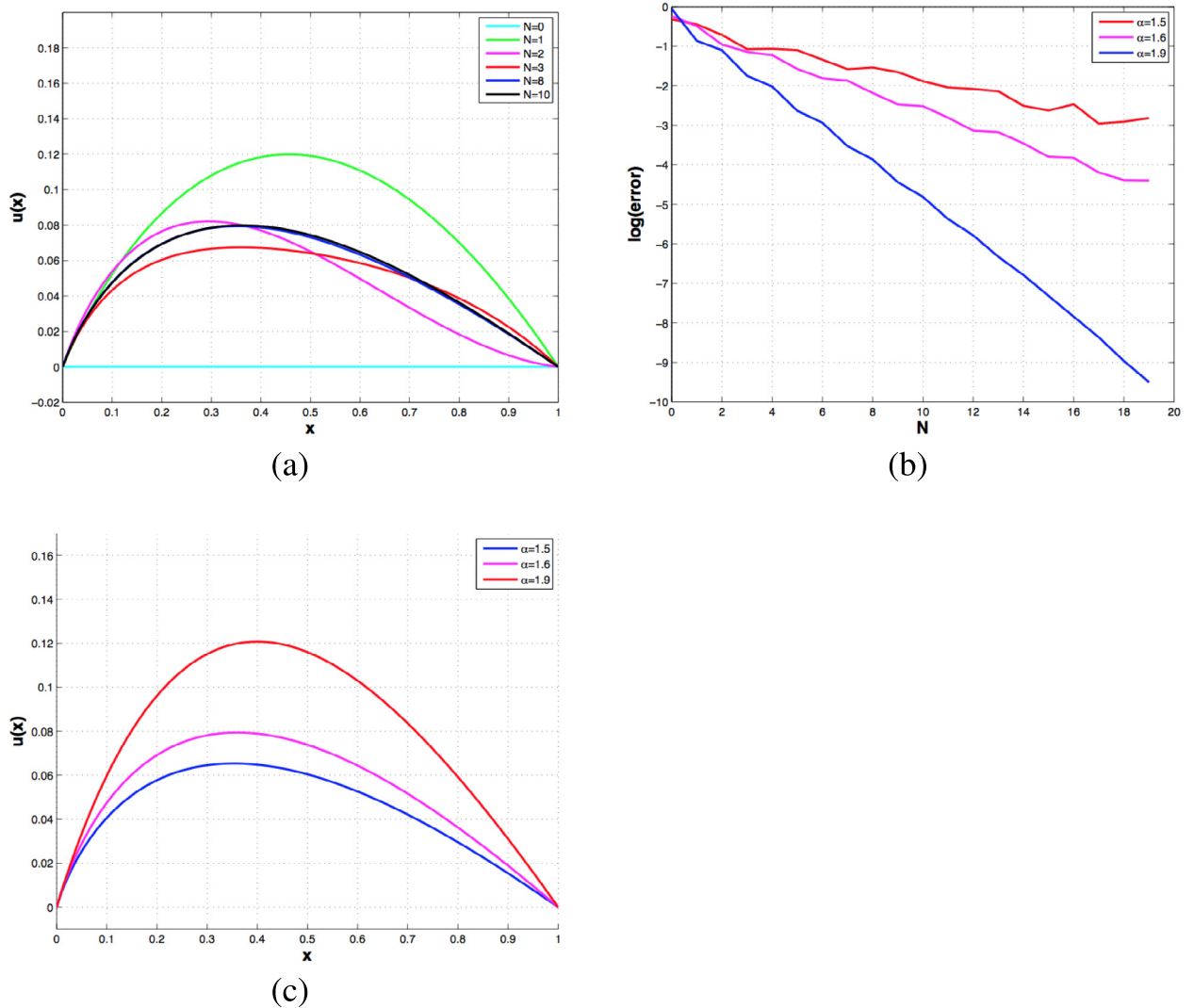


Fig. 7. Panel (a) displays the convergence of HPM for the fractional Gelfand–Bratu model with damping (59) with $\epsilon = 1$ for the case $\alpha = 1.6$ as a function of N , panel (b) shows the dependence of the convergence rate on the fractional derivative α in the model, and panel (c) indicates the differences in solution behavior for three values of α for $\epsilon = 1$.

of successive HPM approximations. These confirm clearly the convergence of HPM and its possible divergence in Table 4. In Table 5, we consider the case with $\alpha = 1.5$ for $\mu = 1$ and $A = 1$. If we compare the results in Tables 2 and 5, we conclude that HPM needs more steps for the fractional case than the ordinary case to reach a similar accuracy. The HPM solutions for different values of α are also given in Fig. 3. Fig. 3(c) shows that HPM may converge to a non-existing solution, here for the values $\lambda = 4$ and $\alpha = 2$. Fig. 3(d) displays a bifurcation diagram for this model. It remains unclear what would happen with the second solution for $1 < \alpha < 2$. In Fig. 4 the effect of changing the parameter A on the convergence in the initial approximation of HPM is displayed.

5.4. Example 5: a fractional Gelfand–Bratu model with damping

Similar to the description in [20], we consider the following nonlinear equation:

$$\begin{cases} \epsilon \mathcal{D}_C^\alpha u + 2u' + 1 + u + \frac{1}{2}u^2 = 0, & 0 < \epsilon \leq 1, \\ u(0) = u(1) = 0. \end{cases} \tag{59}$$

This example includes a damping term and a quadratic approximation to the exponential compared to the previous example. Note that for $\alpha = 2$, there are two solutions for this model, but HPM can only produce one of them. Figs. 5–7 show different scenarios of the model. These are explained in the captions of the figures. The non-uniqueness of the solution is displayed for $\epsilon = 0.35$ and $\alpha = 2$: Fig. 6(a) and (b) were produced using a shooting method with Matlab. The right plot shows the two

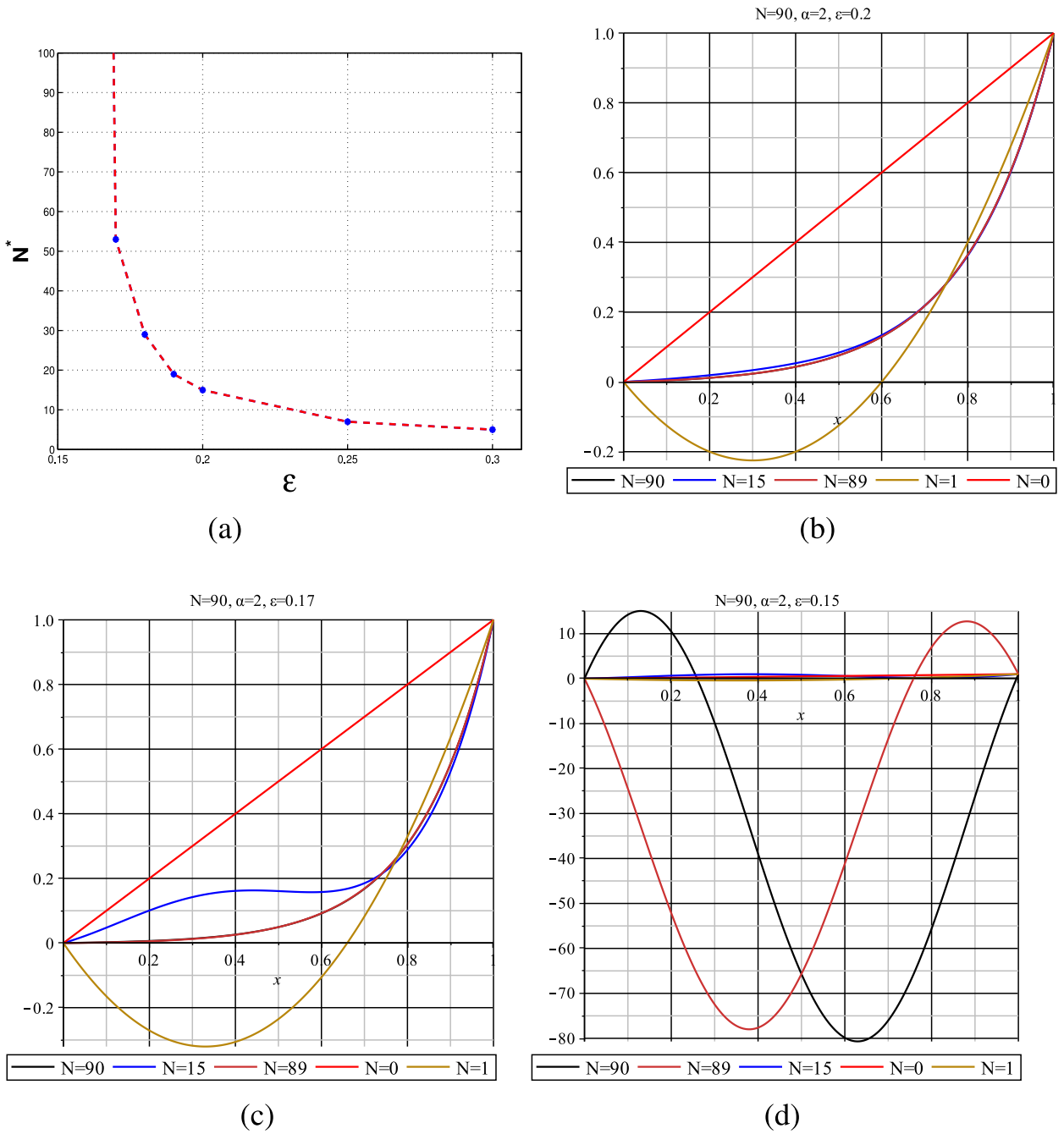


Fig. 8. Panel (a) shows the convergence of HPM depending on the parameter ϵ in the fractional boundary layer model (60). Panel (b)-(d) show convergent and divergent solutions according to the value of ϵ .

curves (in red and blue) in the phase plane $(u, du/dx)$. It can also be clearly observed that the performance of HPM is very sensitive to the choice of the parameter ϵ in the model. Smaller values of ϵ slow down the convergence rate of the method dramatically (see Fig. 5(d)).

5.5. Example 6: a fractional boundary layer model

Our next example is a fractional boundary layer model:

$$\begin{aligned} \epsilon \mathcal{D}_C^\alpha u + \gamma u' &= 0, & 0 < \epsilon \leq 1, & \quad \gamma > 0, \\ u(0) = 0, & u(1) = 1. \end{aligned} \tag{60}$$

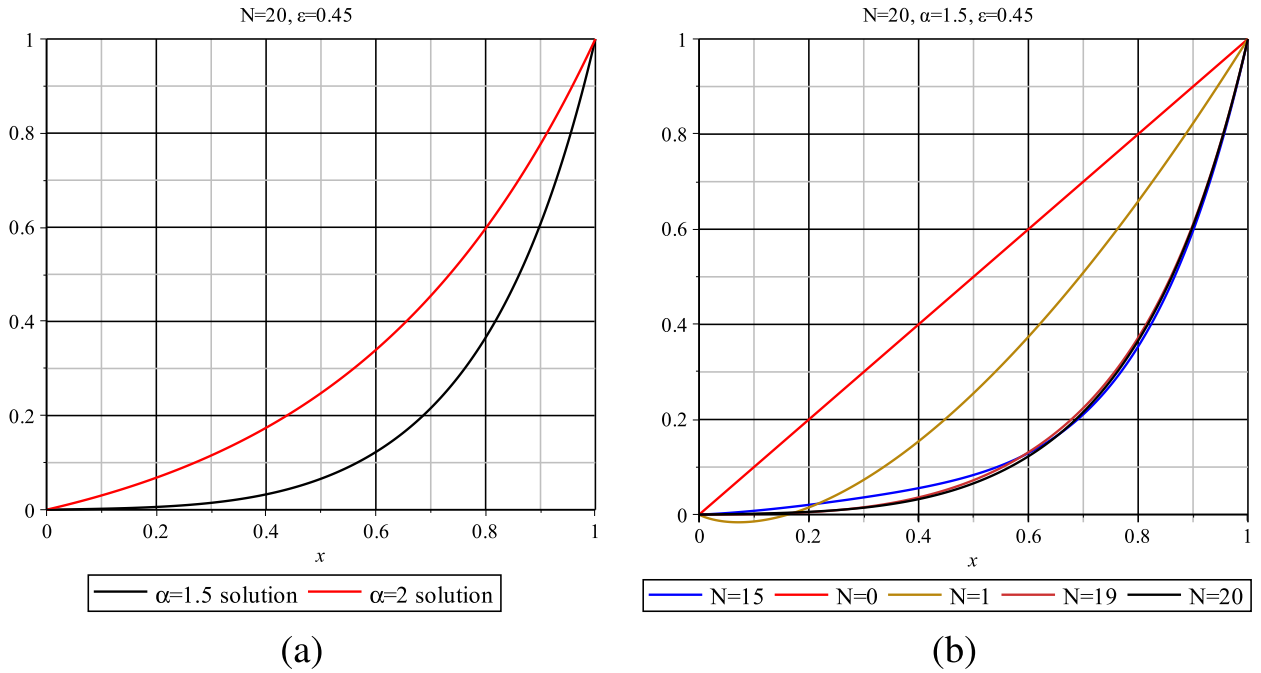


Fig. 9. The effect of varying the fractional order in the fractional boundary layer model (60) is depicted for a fixed value of $\epsilon = 0.45$. The right plot shows the fast convergence of HPM for $\alpha = 1.5$. The left plot displays the difference in solution behavior between the non-fractional $\alpha = 2$ and fractional $\alpha = 1.5$ case.

Table 4
Errors in example 4 for $A = 5$, $\mu = 5$ and $\alpha = 2$.

N	Maximum error	Ratio test
1	0.38411458	0.307292
2	0.39087528	1.017601
3	0.44169314	1.130010
4	0.52929314	1.198328
5	0.66284949	1.252330
6	0.85925246	1.296301
...
23	500.269910	1.519908
24	762.342906	1.523863
25	1164.49295	1.527519

For $\alpha = 2$ and $\gamma = -1$, it has an exact solution:

$$u(x) = \frac{e^x - 1}{e^1 - 1}. \tag{61}$$

In Fig. 8, we present the effect of ϵ on the convergence of the HPM method for $\alpha = 2$. It can be clearly seen that it depends on the small parameter ϵ : for smaller values of ϵ it converges slower or even diverges. This can be seen in Fig. 8(a) where we display the dependence of the value N (denoted by N^*) to obtain a similar accuracy equal to 0.01. Fig. 9 shows HPM solutions for the fractional cases $\alpha = 1.7$ and $\alpha = 1.5$ with $\epsilon = 1.0$. Lower values of α tend to make the solution steeper for a fixed ϵ , but also let HPM converge slower.

6. Summary

In this paper we analyzed the Homotopy perturbation method (HPM) for fractional advection-diffusion-reaction equations. We showed the equivalence between HPM and ADM. A general expression for the coefficients in the series was derived in the case of a nonlinear source term. We applied HPM to a test set of models, both linear and nonlinear. Numerical experiments demonstrated the capability of HPM to find solutions up to high accuracy. However, in some cases the method converged slowly or even diverged. In the situation of non-existing or multiple solutions, HPM may converge to a non-existing one or has difficulties to find the second solution. Finally, the performance of HPM highly depends on the model parameters in the advection-diffusion-reaction equation.

Table 5Errors in example 4 for $A = 1$, $\mu = 1$ and $\alpha = 1.5$.

N	Maximum Error	Ratio Test
1	0.02809378	0.133318
2	0.00582333	0.214116
3	0.00136224	0.241065
4	0.00034055	1.627578
5	0.00008814	1.220158
6	0.00002348	0.737494
7	0.00000632	0.649958
8	0.00000171	0.654176
9	$4.62559720 \cdot 10^{-7}$	0.744348
10	$1.25587544 \cdot 10^{-7}$	1.113443

Acknowledgments

I. Ateş gratefully acknowledges financial support from The Republic of Turkey Ministry of National Education.

References

- [1] J.-H. He, Homotopy perturbation technique, *Comput. Methods Appl. Mech. Eng.* 178 (3–4) (1999) 257–262.
- [2] J.-H. He, Homotopy perturbation method: a new nonlinear analytical technique, *Appl. Math. Comput.* 135 (1) (2003) 73–79.
- [3] J.-H. He, Homotopy perturbation method for solving boundary value problems, *Phys. Lett. A* 350 (1–2) (2006) 87–88.
- [4] J.H. He, New interpretation of homotopy perturbation method, *Appl. Math. Comput.* 20 (18) (2006) 2561–2568.
- [5] H. Jafari, V. Daftardar-Gejji, Positive solutions of nonlinear fractional boundary value problems using adomian decomposition method, *Appl. Math. Comput.* 180 (2006) 700–706.
- [6] S. Momani, Z. Odibat, Comparison between the homotopy perturbation method and the variational iteration method for linear fractional partial differential equations, *Comput. Math. Appl.* 54 (7–8) (2007) 910–919.
- [7] K. Parand, J.A. Rad, Exp-function method for some nonlinear PDE's and a nonlinear ODE's, *J. King Saud Univ. - Sci.* 24 (1) (2012) 1–10.
- [8] S. Liao, *Beyond Perturbation: Introduction to the Homotopy Analysis Method*, CRC Press LLC, 2004.
- [9] S. Liao, *Homotopy Analysis Method in Nonlinear Differential Equations*, Higher Education Press, 2012.
- [10] X.J. Yang, H.M. Srivastava, C. Cattani, Local fractional homotopy perturbation method for solving fractal partial differential equations arising in mathematical physics, *Romanian Rep. Phys.* 67 (3) (2015) 752–761.
- [11] Y. Zhang, C. Cattani, X.J. Yang, Local fractional homotopy perturbation method for solving non-homogeneous heat conduction equations in fractal domains, *Entropy* 17 (2015) 6753–6764.
- [12] M. Sheikholeslami, H.R. Ashorynejad, D.D. Ganji, A. Kolahdooz, Investigation of rotating MHD viscous flow and heat transfer between stretching and porous surfaces using analytical method, *Math. Problems Eng.* 2011 (2011) 17.
- [13] M. Sheikholeslami, D.D. Ganji, Heat transfer of cu-water nanofluid flow between parallel plates, *Powder Technol.* 235 (2013) 873–879.
- [14] I. Podlubny, *Fractional Differential Equations: An Introduction to Fractional Derivatives, Fractional Differential Equations, Some Methods of Their Solution and Some of Their Applications*, Academic Press, San Diego-Boston-New York-London-Tokyo-Toronto, 1999.
- [15] S.G. Samko, A.A. Kilbas, O.I. Marichev, *Fractional Integrals and Derivatives: Theory and Applications*, 1st edition, CRC Press, 1993.
- [16] K.B. Oldham, J. Spanier, *The Fractional Calculus: Theory and Applications of Differentiation and Integration to Arbitrary Order*, Dover Books on Mathematics, 1974.
- [17] X.J. Yang, *Advanced Local Fractional Calculus and Its Applications*, World Science Publisher, New York, 2004.
- [18] G. Jumarie, Modified riemann-liouville derivative and fractional taylor series of nondifferentiable functions further results, *Comput. Math. Appl.* 51 (9–10) (2006) 1367–1376.
- [19] J.-H. He, A tutorial review on fractal spacetime and fractional calculus, *Int. J. Theor. Phys.* 53 (11) (2014) 3698–3718.
- [20] T. Bakri, Y.A. Kuznetsov, F. Verhulst, E. Doedel, Multiple solutions of a generalized singular perturbed bratu problem, *Int. J. Bifurc. Chaos* V22 (N4) (2012).
- [21] S.A. Khuri, A new approach to Bratu's problem, *Appl. Math. Comput.* 147 (2004) 131–136.
- [22] M.I. Syam, A. Hamdan, An efficient method for solving Bratu equations, *Appl. Math. Comput.* 176 (2) (2006) 704–713.
- [23] M. Turkyilmazoglu, Convergence of the homotopy perturbation method, *Int. J. Nonlinear Sci. Numer. Simul.* V12 (2011) 9–14.
- [24] V.G. Kac, A.K. Raina, *Bombay lectures on highest weight representations of infinite dimensional lie algebras*, Advanced Series in Mathematical Physics, 2nd edition, World Scientific, 1987.
- [25] A. Wazwaz, Adomian decomposition method for a reliable treatment of the bratu-type equations, *Int. J. Modern Phys. B* 166 (2005) 652–663.
- [26] E. Babolian, A.R. Vahidi, Z. Azimzadeh, A comparison between the homotopy perturbation method and Adomian's decomposition method for solving nonlinear volterra integral equations, *J. Sci. Tarbiat Univ.* V11 (2) (2012).
- [27] G. Adomian, A review of the decomposition method in applied mathematics, *J. Math. Anal. Appl.* 135 (1998) 501–544.
- [28] J. Biazar, G. Ghazvini, Convergence of the homotopy perturbation method for partial differential equations, *Nonlinear Anal.: Real World Appl.* 10 (5) (2009) 2633–2640.
- [29] J. Biazar, H. Ghazvini, Convergence of the homotopy perturbation method for partial differential equations, *Nonlinear Anal.: Real World Appl.* 10 (5) (2009) 2633–2640.